Available online at www.sciencedirect.com
ScienceDirect
Bioelectrochemistry 69 (2006) 223–233
Bioelectrochemistry
www.elsevier.com/locate/bioelechem

Oxidation chemistry of 2′-deoxyadenosine at pyrolytic graphite electrode

Rajendra N. Goyal *, Aikta Dhawan

Department of Chemistry, Indian Institute of Technology Roorkee, Roorkee-247 667, India

Received 10 January 2006; received in revised form 27 February 2006; accepted 15 March 2006
Available online 3 May 2006

Abstract

The electrochemical oxidation of 2′-deoxyadenosine has been investigated in phosphate containing supporting electrolytes in pH range 2–10 at a pyrolytic graphite electrode by cyclic sweep voltammetry, spectral studies, controlled potential electrolysis and related techniques. The oxidation of 2′-deoxyadenosine occurred in a single well-defined oxidation peak (I_a), over the entire pH range. The electrooxidation occurred by the loss of 6.0±0.5 e^- per mole over the entire pH range. The kinetics of the decay of the UV-absorbing intermediates has been studied and found to follow pseudo first order kinetics having rate constant (k) in the range $(5.7–7.7)\times10^{-4}$ s^{-1}. The major products of electrooxidation were separated by HPLC and characterized by GC–MS/MS, ^{1}H NMR and a tentative mechanism for electrooxidation of 2′-deoxyadenosine has been suggested.

Keywords: 2′-deoxyadenosine; Purine nucleosides; Electrochemical oxidation

1. Introduction

2′-Deoxyadenosine is one of the purine 2′-deoxyribonucleosides present in DNA. It is a carbohydrate derivative of adenine (a nitrogeneous base) in which adenine is linked through its N-9 position via a *N*-glycosidic β-D-*erythro*-pentofuranose β bond to 2′-deoxy-D-ribose [1].

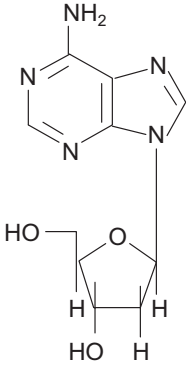

(I)

Certain marine sponges and dorid nudibranch have also been found to contain 2′-deoxyadenosine as the free 2′-deoxyribonucleoside [2]. 2′-Deoxyadenosine is claimed as useful precursor in the synthesis of a wide variety of antiviral, antitumor and antileukemic drugs [3] and [4] and has also exhibited a cardioprotective action [5]. 2′-Deoxyadenosine offers an effective tool for removing nonneuronal cells from neuronal cultures by selectively killing nonneuronal cells without an adverse effect on the viability of sensory dorsal root ganglion neurons and parasympathetic ciliary ganglion neurons [6]. The radical oxidation of adenine moiety of 2′-deoxyadenosine yielded 2-hydroxy-2′-deoxyadenosine in low concentration as compared to 8-oxo-7,8-dihydro-2′-deoxyadenosine [7]. The interaction of 2′-deoxyadenosine with antitumor drug menadione has been studied in organic solvents and micellar medium to eluciate the mechanism of drug-nucleoside interaction and to determine the environmental effects [8]. In view of the importance of 2′-deoxyadenosine in human physiology, simultaneous measurement of 8-oxo-7,8-dihydro-2′-deoxyadenosine and 8-oxo-7,8-dihydro-2′-deoxyguanosine has been made in DNA by HPLC and mass spectrometry [9].

In view of the importance of adenine in the human physiology, an attempt has been made to study the electrochemical oxidation of 2′-deoxyadenosine (**I**) in this paper. It is expected that the results obtained from the electrooxidation of 2′-

* Corresponding author. Tel.: +91 1332 285794; fax: +91 1332 273560.
E-mail address: rngcyfcy@iitr.ernet.in (R.N. Goyal).

1567-5394/$ - see front matter © 2006 Elsevier B.V. All rights reserved.
doi:10.1016/j.bioelechem.2006.03.003

deoxyadenosine will provide deep insights into the redox chemistry of 2′-deoxyribonucleoside of adenine.

2. Experimental

2.1. Materials and instrumentation

2′-deoxyadenosine (**I**) obtained from Fluka Chemie GmbH, Switzerland was used as received. *N*,*N*-bis(trimethyl)triflouroacetamide (BSTFA) was obtained from Sigma and silylation grade acetonitrile was a product of Pierce Chemical Co., Rockford, USA. All other chemicals used were of analytical grade. The pyrolytic graphite electrode (PGE) (~12 mm^2) used as the working electrode for the electrooxidation studies was prepared in the laboratory by the reported method [10]. After each voltammogram the PGE surface was cleaned to remove the adsorbed material by rubbing it on an emery paper. The surface was then washed with distilled water and dried by touching it on soft tissue paper. This procedure resulted in a significantly new surface for each run and showed a variation of ~±10% in peak currents in repeated runs. Hence, for determining the peak current values an average of at least three runs was taken. Voltammetric studies were performed on BAS CV 50 W voltammetric analyzer and recorded in phosphate buffers [11]. Controlled potential electrooxidation was carried out in a conventional H-cell equipped with a three electrode system having a cylindrical platinum gauge as the counter electrode, silver–silver chloride as a reference electrode and a pyrolytic graphite plate (6×1 cm^2) as a working electrode.

UV/Vis spectral changes associated with the electron transfer of 2′-deoxyadenosine at a PGE were carried out in 1 cm quartz cell using Perkin-Elmer-Lambda 35 UV/Vis spectrophotometer. Thin layer chromatography was performed using glass plates coated with silica gel-G using benzene–methanol (4:1) as the solvent. Gas chromatography/mass spectrometric analysis (GC–MS) of the silylated samples was performed with Perkin Elmer Clares 500 Spectrometer in EI mode at 70 eV and High performance liquid chromatographic analysis was carried out using Agilent 1 100 Series HPLC system having a octadecylsilane reversed phase column (7.8×300 mm). For separation of the electrooxidation products of (**I**), several injections of ~300 μl were injected onto the column. FT-IR spectrum of the products was recorded on a Perkin Elmer 1600 series FT-IR spectrophotometer using KBr pellets. The ^{1}H NMR spectrum of the products was recorded in DMSO-d_6, with TMS as internal standard using Brucker dpx 300, NMR spectrometer (300 MHz). Chemical shifts (δ) are reported in parts per million (ppm) of the applied field and coupling constants (J) are expressed in Hertz (Hz).

2.2. Procedure

For recording voltammograms, a stock solution (1 mM) of compound I was prepared in doubly distilled water. The stock solution 2.0 ml was then mixed with 2.0 ml phosphate buffer of ionic strength (μ=1 M) of desired pH so that overall ionic strength of the solution became 0.5 M. The solutions were deaerated for 12–15 min by passing nitrogen gas and voltammograms were then recorded. The coulometric experiments were carried out by the electrooxidation of compound (**I**) in phosphate buffer of desired pH at the peak potential and the value of (n), the number of the electrons involved in the oxidation were determined by the graphical integration of the current–time curve [12].

The progress of the electrolysis was monitored by recording spectral changes at different time intervals. For this purpose, electrolysis was carried out in H-cell at a potential of the oxidation peak (I_a). For recording the UV/Vis spectrum, about 2–3 ml of the solution from the electrolysis cell was transferred each time to a 1 cm quartz cell and the spectrum was recorded in the range 200–400 nm. In the second set of experiments, when the absorbance at λ_{max} was reduced to 50%, the applied circuit was opened and the spectral changes of the solution were monitored at different time intervals. The kinetics of decay of the UV-absorbing intermediates generated during oxidation was recorded at selected wavelengths by monitoring the change in absorbance with time.

The products of the electrooxidation of 2′-deoxyadenosine were characterized at pH=7.20 and pH=3.17 by exhaustively electrolyzing, ~15–20 mg of compound (**I**) at the peak potential (I_a). The progress of electrolysis was monitored by recording UV/Vis at different time intervals. When the oxidation peak (I_a) completely disappeared (generally 24–30 h), the electrolyzed solution was removed from the cell, filtered, lyophilized and extracted using methanol. The products of electrolysis were separated by HPLC and further characterized by m.p., IR, ^{1}H NMR and mass spectrum. For analysis by GC–MS the eluted material under the chromatographic peaks were converted to their trimethylsilyl derivatives. The silylation was carried out in a 3.0 ml vial. For this purpose, 100 μg of the sample, acetonitrile (100 μl) and BSTFA (100 μl) were mixed and heated in an oil bath to 110 °C for about 12–15 min with constant shaking [13]. After cooling at room temperature 2 μl of the silylated sample was injected in GC–MS. In few cases silylation at 140 °C was also carried out for 15 min, so that the glycosidic linkage is hydrolyzed.

3. Results and discussion

3.1. Electrochemical oxidation

Initial studies on voltammetric oxidation were carried out using glassy carbon or platinum as working electrode. However, at these electrodes no oxidation peak was noticed. Hence pyrolytic graphite electrode was used as working electrode which has a large window available for oxidation and also has strong tendency to adsorb purines and its derivatives. In cyclic sweep voltammetry at a sweep rate (v=100 mV/s), 0.5 mM solution of 2′-deoxyadenosine exhibited a single well-defined oxidation peak (I_a) at PGE over the entire pH range studied, when the sweep was initiated in the positive direction. In the reverse sweep a cathodic peak (II_c) was observed only over the pH range 7–10. In the second sweep towards positive potentials two oxidation peaks (II_a), (III_a) were observed in the pH range 7–10 at a potential less positive than that of peak (I_a). Peak (II_a)

Table 1
Effect of sweep rate on the peak current of peaks II_c and II_a of 2′-deoxyadenosine at pH=7.20 at a PGE

Sweep rate, v/mV s^{-1}	Peak current/μA		II_c/II_a *
	II_c	II_a	
20	23.52	23.98	0.98
50	37.15	37.94	0.98
100	48.08	49.14	0.98
200	76.87	75.77	1.01
300	114.90	117.0	0.98
400	146.20	144.9	1.01

* Average of at least three replicate determinations.

formed a quasi-reversible couple with the peak (II_c). The ratio of the peak currents for peak II_c/II_a were close to 1.0 over the entire sweep region as presented in Table 1, indicating thereby the quasireversible nature of the redox couple. A typical cyclic voltammogram of 2′-deoxyadenosine is presented in Fig. 1.

The peak potentials of the oxidation peaks (I_a), (II_a), (III_a) and (II_c) were dependent on pH and shifted to less positive potential with increase in pH. This behavior indicated the involvement of protons in the electrode process. The E_p versus pH plots for these oxidation and reduction peaks were linear and the dependence of E_p on pH using linear regression analysis can be expressed by the following relations with a correlation coefficient of ~0.9936, ~0.9803, ~0.9978 and ~0.9947 respectively.

$$E_p(2-10) = (1633.4-58.700\ \mathrm{pH})\ \mathrm{mV\ versus\ Ag/AgCl} \quad (\mathrm{peak}(I_a))$$

$$E_p(7-10) = (557-58.853\ \mathrm{pH})\ \mathrm{mV\ versus\ Ag/AgCl} \quad (\mathrm{peak}(II_a))$$

$$E_p(7-10) = (1075.8-59.029\ \mathrm{pH})\ \mathrm{mV\ versus\ Ag/AgCl} \quad (\mathrm{peak}(III_a))$$

$$E_p(7-10) = (494.51-58.187\ \mathrm{pH})\ \mathrm{mV\ versus\ Ag/AgCl} \quad (\mathrm{peak}(II_c))$$

The peak current for peak (I_a) increased with an increase in concentration of 2′-deoxyadenosine. The plot of i_p vs. concentration was linear in the range 0.1–0.7 mM and at higher concentrations the peak current became constant as presented in Fig. 2. The sweep rate studies were carried in the range of 20–500 mV/s and it was found that the peak current of the oxidation peak (I_a) of 2′-deoxyadenosine increased with an increase in sweep rate. At $v>500$ mV/s the peak merged with the background. Hence, studies at $v>500$ mV/s could not be carried out. The plot of $i_p/\sqrt{v}$ versus log (v/mV s^{-1}) (Fig. 3) indicated that the value of the peak current function increased with an increase in the logarithm of sweep rate. This behavior indicated a strong adsorption of the reactant at the surface of PGE [14]. The effect of the sweep rate on E_p of the peak (I_a) was also studied in the sweep range 20–500 mV/s. The value of E_p shifted to more positive potentials with the increase in v. The

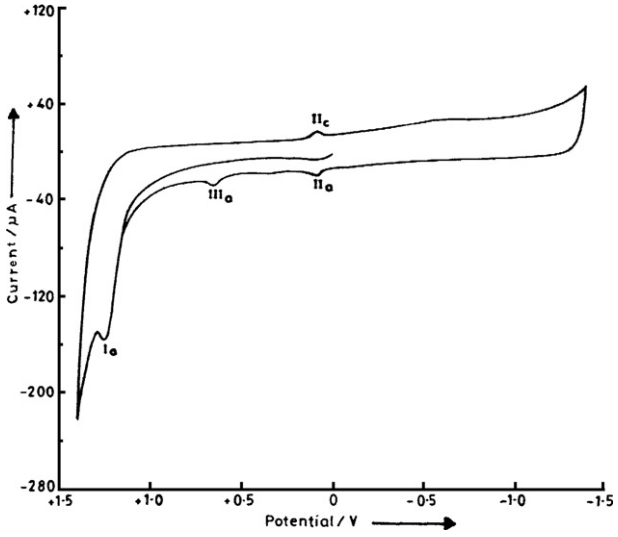

Fig. 1. Typical cyclic voltammograms observed for 0.5 mM 2′-deoxyadenosine at sweep rate=100 mV s^{-1} in phosphate buffers at pH=7.20 at a PGE.

plot of E_p versus log (v/mV s^{-1}) was linear and the dependence can be represented as —

$$E_p(2-10) = (96.802\log v + 1080.9)\ \mathrm{mV\ versus\ Ag/AgCl} \quad (\mathrm{peak}(I_a))$$

with a correlation coefficient of ~0.9896. This behavior is consistent with the EC nature of the reaction in which the electrode reaction is coupled with an irreversible follow-up chemical step [15].

Controlled potential electrolysis of 2′-deoxyadenosine was performed in phosphate buffers at pH=3.17 and pH=7.20 at potential of the oxidation peak (I_a) at PGE. The number of electrons (n) involved in the electrooxidation was determined by monitoring the exponential decay of the current–time curve. The plot of i_p versus time was exponential and average experimental value of number of electrons were ($n=6.0\pm0.5$) per mole over the entire pH range. The value of n may not be precise because of long time required for complete oxidation due to which large background correction was needed.

3.2. Spectral studies

The UV/Vis spectra of 2′-deoxyadenosine were monitored over the entire pH range of 2–10 and two well-defined λ_{max} at 210 and 260 nm were observed. At pH=3.17, Curve 1 in Fig. 4

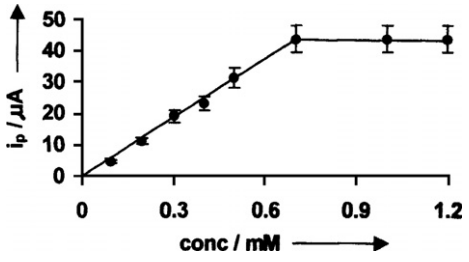

Fig. 2. Dependence of peak current (i_p) of peak I_a on concentration of 2′-deoxyadenosine at pH=7.20, v=100 mV s^{-1} at a PGE.

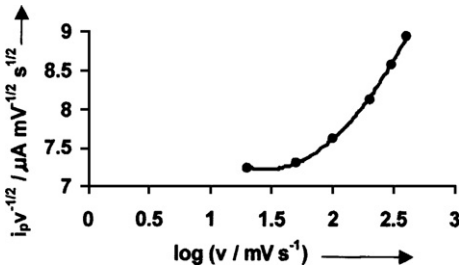

Fig. 3. Dependence of $i_p/\sqrt{v}$ on log (v/mV s^{-1}) for peak I_a of 0.5 mM 2′-deoxyadenosine at pH=7.20 at a PGE.

depicts the initial spectrum of 2′-deoxyadenosine just before the electrooxidation. Upon application of the peak (I_a) potential, the absorbance in the regions 220–240 nm and 280–400 nm increased systematically as presented by the (curves 2–9). However, in the regions 240–280 nm and 200–220 nm the absorbance decreased up to 110 min of electrolysis and then increased. No clear isosbestic points were noticed.

On the other hand at pH=7.20, curve 1 in Fig. 5 shows the initial spectrum of 2′-deoxyadenosine just before the electrooxidation. Upon application of the peak (I_a) potential, the absorbance in the region 200–220 nm first decreased as depicted by the curves 2–8 and then increased (curves 9–11), whereas, in the regions 220–240 nm and 280–350 nm absorbance increased systematically (curves 2–11). On the other hand the absorbance in the region 240–280 nm decreased systematically (curves 2–11). Thus, over the entire pH range no clear isosbestic points were noticed during spectral changes, which indicated the involvement of the competitive chemical reactions at the electrode surface. Moreover, the increase in the absorbance in the longer wavelength region 290–400 nm indicated the formation of more conjugated species during oxidation probably dimers and trimers.

In open circuit relaxation experiments, it was observed that the absorbance in the range 220–400 nm decreased systematically, due to the decay of the intermediates generated during the

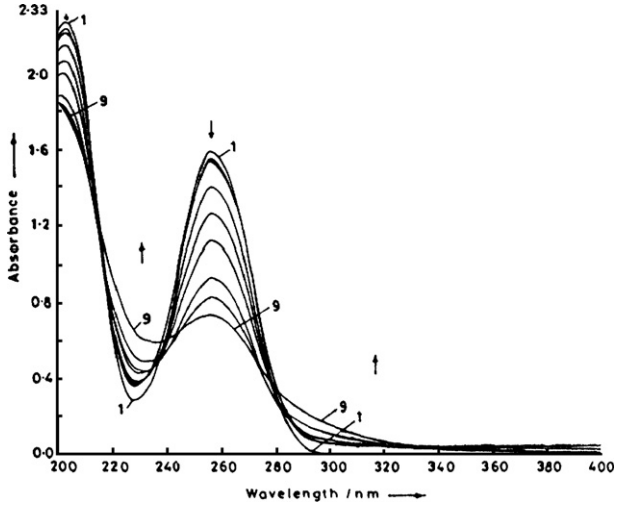

Fig. 4. Spectral changes observed during electrooxidation of 0.5 mM 2′-deoxyadenosine at pH=3.17 at PGE. Curves were recorded at (1) 0 min. (2) 5 min. (3) 10 min. (4) 20 min. (5) 30 min. (6) 45 min. (7) 60 min. (8) 80 min. (9) 110 min. of electrolysis.

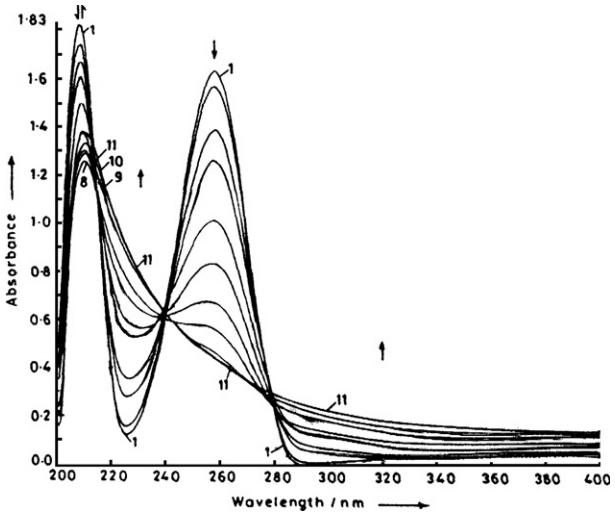

Fig. 5. Spectral changes observed during electrooxidation of 0.5 mM 2′-deoxyadenosine at pH=7.20 at PGE. Curves were recorded at (1) 0 min. (2) 5 min. (3) 10 min. (4) 20 min. (5) 30 min. (6) 45 min. (7) 60 min. (8) 80 min. (9) 100 min. (10) 130 min. (11) 160 min. of electrolysis.

electrooxidation. The kinetics of the decay of the UV/Vis absorbing intermediate generated were monitored by recording the changes in the absorbance at selected wavelengths (225, 260 and 300 nm) as a function of time. The absorbance versus time plots at different wavelengths showed an exponential decay (Fig. 6) and the plot of log (A–A_∞) versus time (where A_∞ and A are the absorbance at infinite time and at the reaction time respectively) were linear (inset, Fig. 6). The values of the pseudo first-order rate constant (k) were determined at different pHs as presented in Table 2. The change in the absorption clearly indicates that the purine ring of 2′-deoxyadenosine is likely to be destroyed during the electrooxidation. The formation of the dimers and trimers as the products, are most likely to be the minor products of the total oxidation pathway.

3.3. Product characterization

The products of the electrooxidation of 2′-deoxyadenosine were characterized at pH=3.17 and pH=7.20. The complete

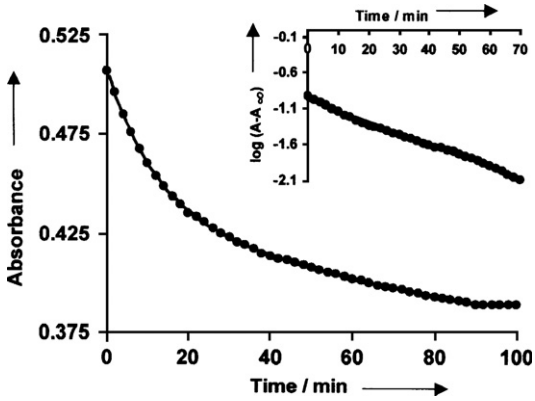

Fig. 6. Plot of absorbance versus time and log (A–A_∞) vs. time (inset) plot measured at 225 nm for the first-order decay of the UV-absorbing intermediate generated during electrooxidation of 0.5 mM 2′-deoxyadenosine at a PGE, pH=7.20.

Table 2
Observed k values for the decomposition of the UV–vis absorbing intermediate generated during electrooxidation of 2′-deoxyadenosine at a PGE

pH	λ/nm	Rate constant/$k\times10^{-4}$ s^{-1} *
3.17	225	7.7
	260	7.6
	300	7.7
5.11	225	7.7
	260	7.7
	300	7.7
7.20	225	5.8
	260	5.7
	300	5.8
9.12	225	6.3
	260	5.8
	300	5.9

* Average of at least three replicate determinations.

oxidation of 2′-deoxyadenosine leading to the formation of several stable products took ~24–30 h of the electrolysis. The exhaustively electrolyzed solution of 2′-deoxyadenosine were lyophilized and extracted using methanol. The material obtained at pH=3.17 exhibited four spots in TLC (R_f=0.32, 0.40, 0.45 and 0.55) whereas the material obtained at pH=7.20 exhibited three spots (R_f=0.28, 0.57 and 0.65). For the determination of the molar masses of the different constituents of exhaustively electrolyzed samples, the products were converted to their thermally stable, volatile trimethylsilyl derivatives. The GC–MS analysis of the silylated samples was performed and five major peaks were detected at pH=3.17 at retention times R_t~5.29, 6.26, 9.86, 11.05 and 19.09 min having m/z 448 (M^+), 464 (M^+), 964 (M^+), 948 (M^+) and 932 (M^+) respectively whereas GC–MS chromatogram of the silylated material at pH=7.20 gave four clear peaks at R_t~6.018, 8.697, 9.952 and 17.957 min having m/z 350 (M^+), 518 (M^+), 908 (M^+) and 950 ($M+H^+$) respectively. The data giving m/z values and the relative abundance of the high-mass fragments in the mass spectrum have been summarized in Tables 3 and 4 respectively (supplementary file). The high-mass peaks and the fragmentation pattern clearly supported the proposed products of electrooxidative pathway.

3.4. Silylation at 140 °C at pH=3.17

To further support the molar masses of the proposed dimers/trimers, the freeze-dried brownish colored material at pH=3.17 was silylated with BSTFA/acetonitrile at a higher temperature (140 °C). It was interesting to observe that on exposure to such a high temperature, all the 2-deoxyribose moieties were hydrolyzed due to the cleavage of *N*-glycosidic-D-*erythro*-pentofuranose-β bond during silylation. The GC–MS chromatogram now gave major peaks at R_t~4.21, 6.16, 8.17, 14.56 and 18.17 min having m/z 448 (M^+), 350 (M^+), 732 (M^+), 717 ($M+H^+$) and 700 (M^+) respectively. Interestingly, due to the loss of the sugar units NH_2 group from the adenine base upon silylation changes to $N[Si(CH_3)_3]_2$. Thus, these studies further supported the proposed products of the oxidative pathway. The products of the electrooxidation of 2′-deoxyadenosine formed in CPE were also separated by HPLC.

3.5. Products at pH=3.17

The HPLC chromatogram of the products formed in CPE at pH=3.17 exhibited five peaks at retention times R_t~11.955, 16.144, 19.182, 20.617 and 22.914 min (Fig. 7). As the peak (P_2) was very small, the material collected under this peak was never enough to permit its characterization. The details of the lyophilized material collected under the chromatographic peaks P_1, P_3, P_4 and P_5 are as follows:

3.6. HPLC peak 1

The volume eluted under the chromatographic peak P_1 was lyophilized. The colorless material obtained exhibited a single spot in TLC with R_f~0.46 and had a m.p. 274 °C. The prominent peaks obtained in the FT-IR spectrum were at ν_{max}/cm^{-1} 3438, 3424 (NH_2); 3234, 3228, 3156, 3145 (OH); 2925, 2852 (CH); 1691, 1653, 1635, 1612, 1602, 1570, 1511, 1492 (C–N) and (C–C); 1243, 1198, 1174, 1108, 1072, 1025 (C–C). The mass spectrum of its volatile trimethylsilyl derivative exhibited a clear peak at m/z 964 (M^+, 6.98%). The other high-mass peaks observed in the fragmentation pattern supported the product to be C_2–O–O–C_2 bridged dimer (**18**). The ^{1}H NMR spectrum of the material exhibited signals at δ=8.26 (4H, s, 2×NH_2), 7.26 (2H, s, 2×CH). The signals between δ=2.73–3.04 and 4.45–4.95 observed as clusters correspond to the protons of the deoxyribose groups and the integration in these regions indicated a total of 18 protons. As the protons of deoxyribose exhibit signals as a cluster in this region, it is difficult to assign these protons to different H and OH groups. The data further supported the structure of the product formed by the rapid dimerization of radical species (**17**) having odd electron at oxygen atom at C_2 position with its similar moiety and finally forming a dimer (**18**) with peroxide linkage. The presence of peroxide group in the product was also confirmed by the test suggested in the literature [16] and [17] in which 1.0 mL of 10% acidified potassium iodide solution was added to a small amount of the product. A few drops of starch solution were then added and a blue black color was observed in ~1 min.

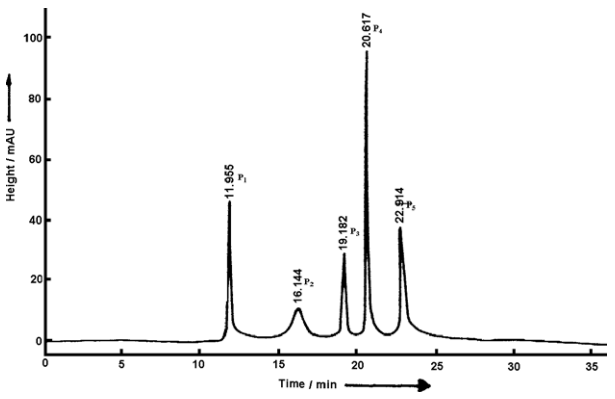

Fig. 7. High performance liquid chromatogram of the electrolyzed products of 2′-deoxyadenosine at PGE, pH=3.17.

3.7. HPLC peak 3

The concentrated methanolic extract of the lyophilized material eluted under the chromatographic peak P_3, exhibited a single spot in TLC with $R_f \sim 0.51$ and had a m.p. 298°C. The prominent peaks obtained in the FT-IR spectrum of the material were at ν_{max}/cm^{-1} 3418, 3412 (NH_2); 3214, 3166 (OH); 2915, 2862 (CH); 1681, 1653, 1630, 1611, 1602, 1590, 1501, 1472 (C═N) and (C═C); 1243, 1200, 1184, 1101, 1076, 1021 (C–C). The mass spectrum of its volatile trimethylsilyl derivative exhibited a clear molar mass peak at *m*/*z* 948 (M^+, 4.58%). The other high-mass peaks observed in the fragmentation pattern supported the product to be C_8–O–C_2 bridged dimer (**20**). The ^{1}H NMR spectrum of the material eluted exhibited signals at $\delta = 8.22$ (2H, s, NH_2), 8.12 (2H, s, NH_2), 7.29 (1H, s, CH), 7.11 (1H, s, CH). The signals between $\delta = 2.82$–3.35 and 5.15–5.51 observed as clusters correspond to the protons of the deoxyribose groups and the integration in these regions indicated a total of 18 protons. The data further supported the structure of the product formed by the rapid coupling of C_8 radical species ($\mathbf{I_d}$) with a radical species (**17**) having odd electron at oxygen atom at C_2 position.

3.8. HPLC peak 4

The white material eluted under this peak exhibited a single spot in TLC $R_f \sim 0.39$ and had a m.p. 238 °C. The mass spectrum of the silylated material exhibited a clear peak at *m*/*z* 448 (M^+, 4.37%) along with a sharp peak at *m*/*z* 433 (M^+–CH_3, 7.86%). Thus, it was concluded that this material had a molar mass of 448, which corresponds to alloxan monohydrate. The IR spectrum of the material gave strong bands at 3200 (N–H), 1678 (cyclic C═O), 1408 (C–H), 1260, 1169, 1020, 864 and 804 (C–N and C–C) and was practically superimposable on that of an authentic sample of alloxan. Thus, the data further supported the structure as alloxan monohydrate.

3.9. HPLC peak 5

The trimethylsilyl derivative of the material eluted under the chromatographic peak P_5 gave a clear peak at *m*/*z* 932 (M^+, 5.22%) in GC–MS data. The material gave a single spot in TLC with $R_f \sim 0.54$ and had a m.p. 286°C. The FT-IR spectrum exhibited broad bands at 3442, 3415 (NH_2); 2944, 2875 (CH); 1672, 1643, 1629, 1615, 1600, 1588, 1503, 1487 (C═N) and (C═C). The ^{1}H NMR of the material exhibited signals at $\delta = 8.09$ (4H, s, $2 \times NH_2$), 7.06 (2H, s, $2 \times$CH). The signals between $\delta = 2.62$–2.95 and 3.89–4.48 observed as clusters correspond to the protons of the deoxyribose groups and the integration in these regions indicated a total of 18 protons and confirmed the material as C_8–C_8 bridged dimer (**22**) formed by the rapid dimerization of C_8 radical species ($\mathbf{1_d}$).

3.10. Products at pH = 7.20

The HPLC chromatogram of the products formed in CPE at pH = 7.20 exhibited five peaks at retention times $R_t \sim 12.057$, 12.204, 15.834, 20.141 and 25.767 min. Due to close retention times peaks P_1 and P_2 could not be separated. Thus, the materials collected under the chromatographic peaks P_3, P_4 and P_5 are characterized as follow:

3.11. HPLC peak 3

The volume collected under the chromatographic peak P_3 was lyophilized and the material so obtained exhibited a single spot in TLC with $R_f \sim 0.55$ and had a m.p. 264 °C. The prominent peaks obtained in the FT-IR spectrum were at ν_{max}/cm^{-1} 3448, 3417 (NH_2); 3278, 3255 (OH); 1598, 1523 (C═C). The mass spectrum of its volatile trimethylsilyl derivative exhibited an intense peak at *m*/*z* 908 (M^+, 5.42%) and thus suggested the silylated material as C_8–O–O–C_8 dimer (**26**). The molar mass of 908 accounts for eight silylable positions in this compound. The other high-mass peaks observed in the fragmentation pattern supported its formation. The ^{1}H NMR spectrum of the component exhibited signals at $\delta = 8.45$ (4H, s, $2 \times NH_2$), 7.43 (2H, s, $2 \times$OH). The signals between $\delta = 2.86$–3.34 and 4.61–5.03 observed as clusters and correspond to the protons of the deoxyribose groups. The integration in these regions indicated a total of 18 protons, which further supported the formation of C_8–O–O–C_8 dimer as one of the products of electrooxidation by the rapid dimerization of the radical species (**24**). The presence of peroxide group in the product was also confirmed as reported for compound (**18**).

3.12. HPLC peak 4

The mass spectrum for this component silylated with BSTFA/acetonitrile exhibited a clear molar mass peak at *m*/*z* 518 (M^+, 6.22%) along with a large peak at *m*/*z* 503 (M^+–CH_3, 42.52%). The molar mass of 518 suggested the structure as pentasilylated allantoin. A comparison of the IR spectrum of the material obtained with an authentic sample of allantoin indicated them to be superimposable. Moreover, TLC indicated a single spot with $R_f \sim 0.25$ and the material had a m.p. 239 °C. The fragmentation pattern of the GC–MS spectrum further supported the material as allantoin.

3.13. HPLC peak 5

The volume collected under the chromatographic peak P_5 was lyophilized. The concentrated material so obtained exhibited a single spot in TLC with $R_f \sim 0.42$ and had a m.p. 279 °C. The prominent peaks obtained in the FT-IR spectrum were at ν_{max}/cm^{-1} 3439, 3420 (NH_2); 1678, 1655, 1622, 1609, 1593, 1582, 1576 (C═N) and (C═C). The mass spectrum of its volatile trimethylsilyl derivative exhibited an intense peak at *m*/*z* 950 ($M+H^+$, 3.8%) and suggested the molar mass as 949, which corresponds to the formation of C_8–N_6–C_8 trimer (**31**). The ^{1}H NMR spectrum of this component exhibited signals at $\delta = 8.34$ (2H, s, NH_2), 8.25 (2H, s, NH_2), 7.96 (1H, d, *J* 5.4, NH), 7.56 (1H, d, *J* 5.4, CH), 7.39 (1H, s, NH), 7.26 (1H, s, CH), 7.10 (1H, s, CH), 7.02 (1H, s, CH). The signals between $\delta = 2.71$–3.42 and 5.26–5.46 observed as clusters correspond to

the protons of the deoxyribose groups and the integration in these regions indicated a total of 9 protons and further supported the material as C_8–N_6–C_8 linked trimer (**30**). The trimer (**30**) has eight silylable sites, however, on silylation it would give a hexasilylated product of molar mass 949 (**31**).

3.14. Redox mechanism

The evidence presented above clearly indicates that the electrooxidation of 2′-deoxyadenosine (**1**) occurs in an overall $6e^-$, $6H^+$ process, corresponding to peak (I_a) in CV. The tentative mechanism assigning the observed anodic and cathodic signals to their corresponding reactions during the electrooxidation of 2′-deoxyadenosine (**1**) at pH=3.17 and pH=7.20 are presented in Schemes 1, 2 and 3 respectively.

On the basis of product characterization it seems reasonable to conclude that the rupture of the imidazole ring occurs in acidic medium and pyrimidine ring of purine nucleoside breaks in neutral medium. Thereby, leading to the formation of alloxan monohydrate and urea deoxyribose as products in acidic pH

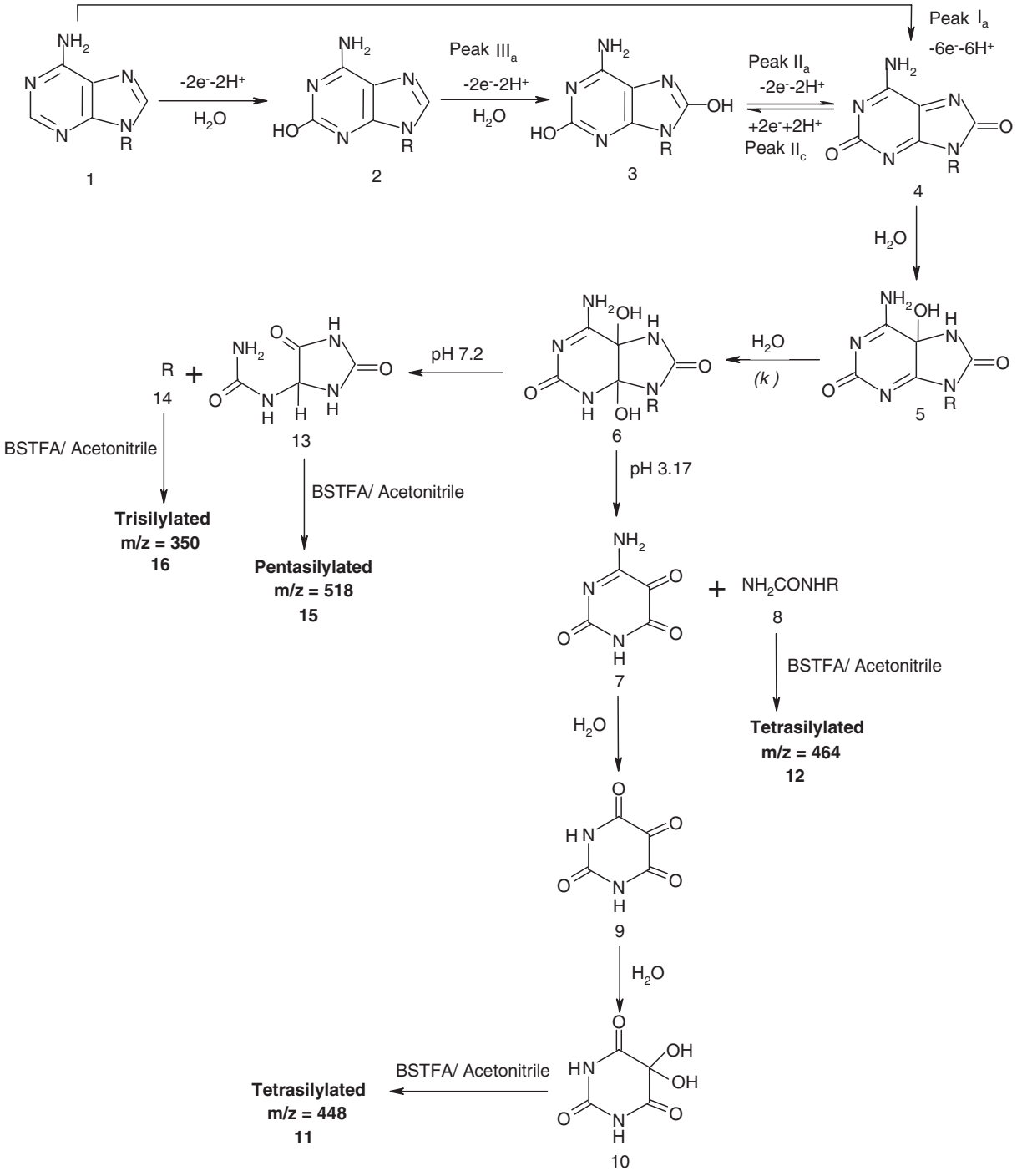

Scheme 1. Tentative mechanistic pathway proposed for the electrooxidation of 2′-deoxyadenosine at pH=3.17 and 7.20.

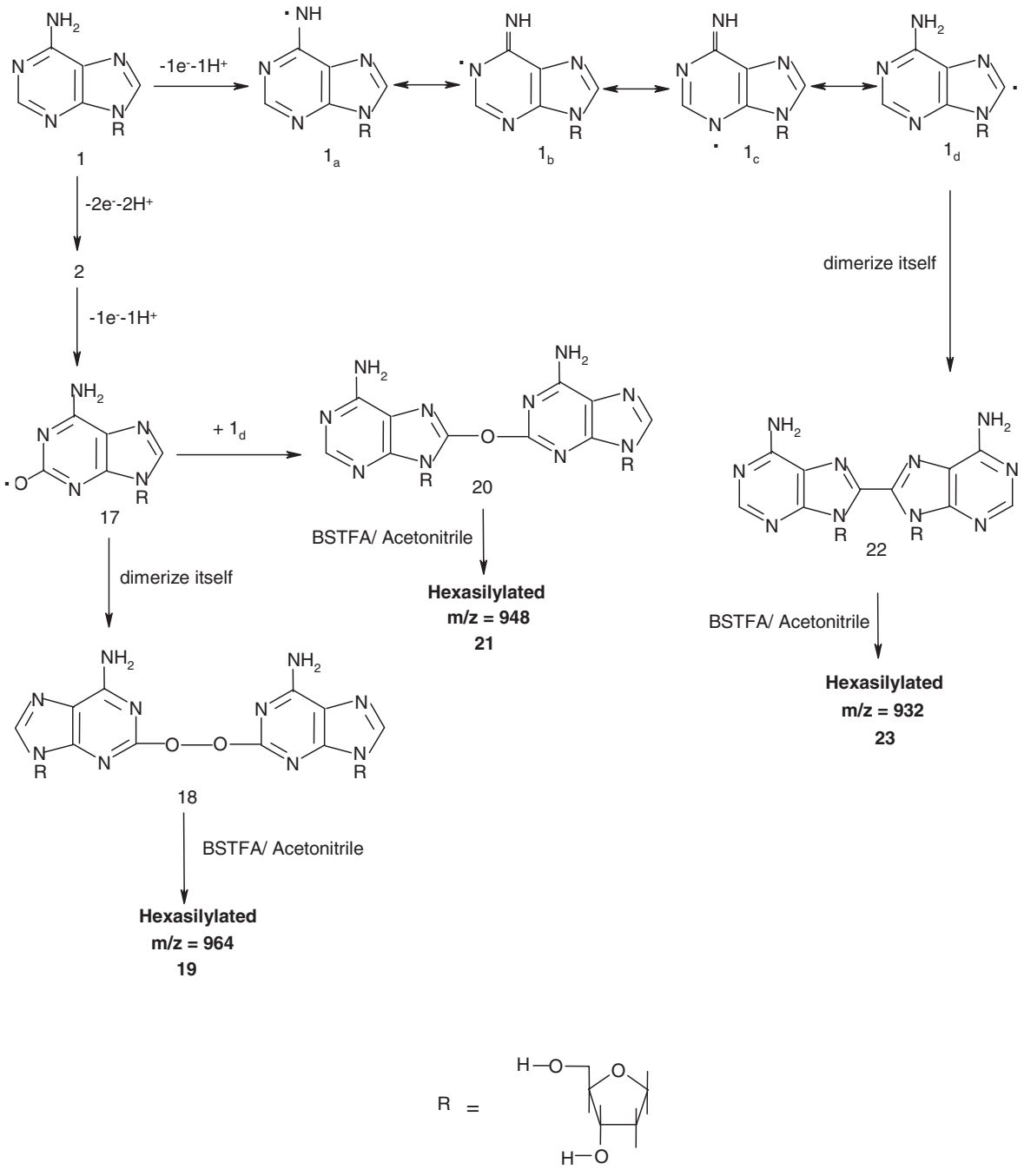

Scheme 2. Tentative mechanistic pathway proposed for the electrooxidation of 2′-deoxyadenosine at pH=3.17.

range whereas allantoin at neutral pH in the primary electrode reactions. The initial $2e^-$, $2H^+$ oxidation of 2′-deoxyadenosine (**1**) can form either 2-hydroxy-or 8-hydroxy-2′-deoxyadenosine. However, on the basis of studies of adenine oxidation reported in the literature [18] and [19], it can be concluded that first $2e^-$, $2H^+$ oxidation will lead to 2-hydroxy-2′-deoxyadenosine (**2**). Further $2e^-$, $2H^+$ oxidation of (**2**) will give 2,8-dihydroxy-2′-deoxyadenosine (**3**). It is well reported in the literature that 2,8-dihydroxy derivatives of adenine gets oxidized at less positive potential in comparison to 2-hydroxyadenine and adenine [18]. Thus, 2,8-dihydroxydeoxyadenosine (**3**) undergoes a further $2e^-$, $2H^+$ oxidation corresponding to peak (II_a) to give diimine species (**4**). Peak (II_c) obtained in CV of 2′-deoxyadenosine appears to be due to the quasi-reversible reduction of the diimine (**4**) to 2,8-dihydroxy-2′-deoxyadenosine (**3**) as presented in Scheme 1. The peak (III_a) corresponds to the oxidation of 2-hydroxy-2′-deoxyadenosine adsorbed on the surface of the microelectrode to 2,8-dihydroxy-2′-deoxyadenosine via $2e^-$, $2H^+$ oxidation step. The diimine species (**4**) obtained during the oxidation of purines have been found to be unstable due to two C═N bonds and its short half life of few ms (~50 ms) has been already documented in the literature [20]. Hence, the diimine species (**4**) is readily attacked by water to give imine alcohol (**5**) in a

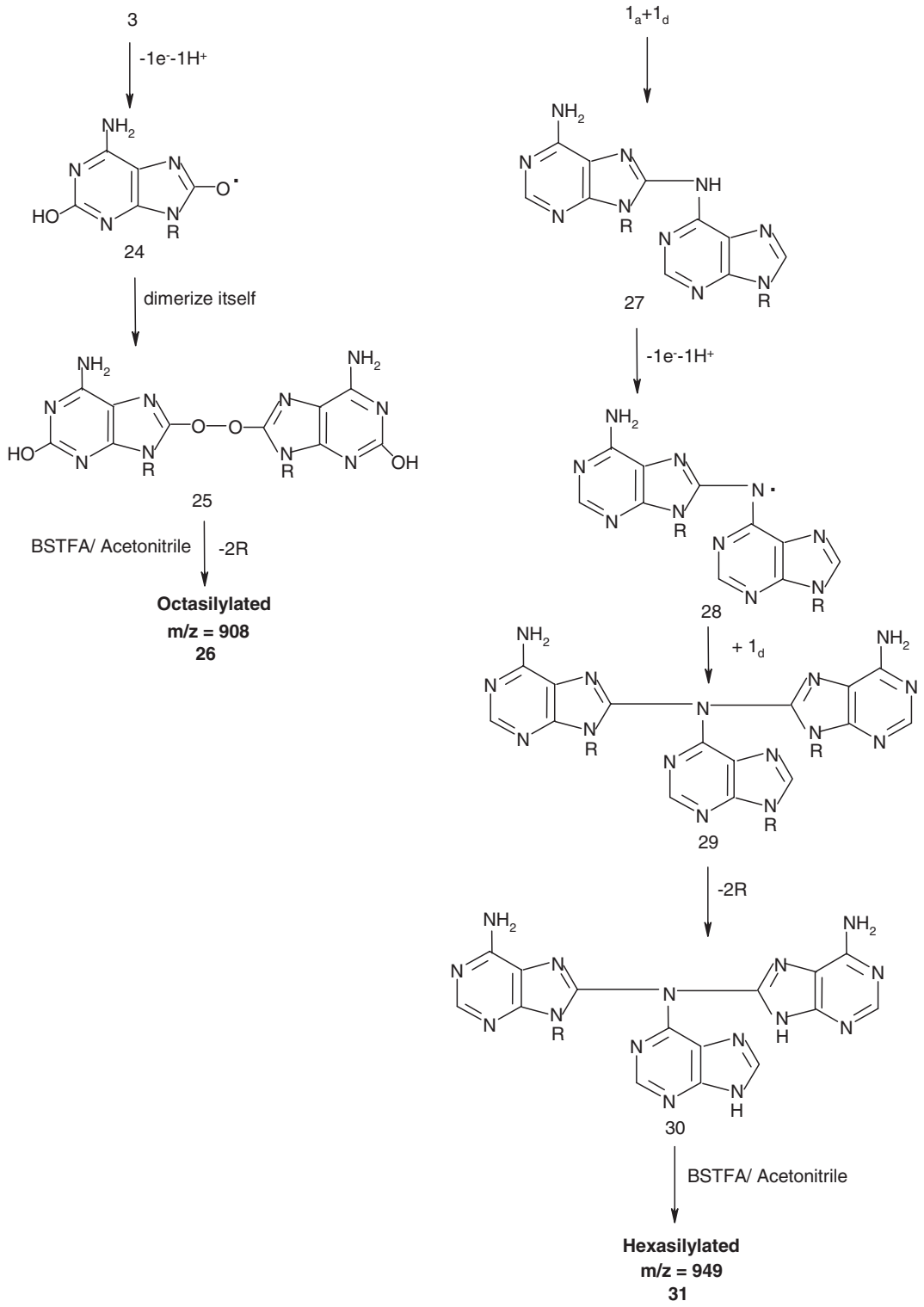

Scheme 3. Tentative mechanistic pathway proposed for the electrooxidation of 2′-deoxyadenosine at pH=7.20.

chemical follow-up step. The attack of second water molecule on (**5**) is a slow process and leads to the formation of diol (**6**). The *k* values observed spectrophotometrically represent the decomposition of imine alcohol (**5**) to diol (**6**) in a pseudo first-order reaction. The cleavage of imidazole ring then occurs to give alloxan monohydrate (**10**) and urea deoxyribose (**8**) as the final product at pH=3.17. However, at pH=7.20 pyrimidine ring breaks to give allantoin (**13**) and deoxyribose (**14**) as the major product as shown in Scheme 1. The rupture of the imidazole ring in acidic media and of the pyrimidine ring in the neutral media during oxidation of purine nucleosides has also been reported by various workers [21] and [22]. Alloxan monohydrate possesses four reactive sites and GC–MS data clearly indicates that all the reactive hydrogen atoms are

replaced with trimethylsilyl groups on silylation with BSTFA/acetonitrile to give tetrasilylated alloxan having *m/z* 448 which was observed in the GC–MS at $R_t \sim 5.29$ min. The formation of tetrasilylated urea deoxyribose can be accounted for, on the basis, of the GC–MS peak at $R_t \sim 6.26$ min having *m/z* 464, which corresponds to M^+ peak of (**12**). The pentasilylated allantoin (**15**) formed as a major product at pH = 7.20, was noticed in GC–MS at $R_t \sim 8.69$ min having *m/z* 518, corresponding to a clear molecular ion (M^+) peak.

The identification of dimers and trimers formed during the oxidation of 2′-deoxyadenosine strongly indicates that the radical–radical coupling reactions also play a significant role. Thus, a parallel pathway also appears to take place for the electrooxidation of 2′-deoxyadenosine (**1**), which involves $1e^-$, $1H^+$ oxidation to give a free radical moiety ($\mathbf{1_a}$). The removal of $1e^-$, $1H^+$ will occur from the amino group at position 6 as has been reported during oxidation of purines [23]. The free radical ($\mathbf{1_a}$) can have several resonating structures as shown in Scheme 2. The free radicals can undergo electrodimerization by any of the mechanism such as radical–radical coupling or radical–substrate coupling as shown in Schemes 2 and 3.

3.14.1. In acidic media

The species ($\mathbf{1_d}$), in which odd electron is present at position 8 seems to rapidly dimerize to give C_8–C_8 bridged dimer (**22**). The mass calculations of the silylated derivative of compound (**22**) (cal. *m/z* 932), corresponding to the GC–MS peak at $R_t \sim 19.09$ min clearly, supported the retention of both the deoxyribose sugar moieties in the dimer (**23**). It was interesting, to observe that upon silylation both the reactive OH groups from the five membered deoxyribose ring are rapidly silylated. In contrast, the NH_2 group from the adenine base, upon silylation changes to $NHSi(CH_3)_3$ rather than $N[Si(CH_3)_3]_2$. Such silylation of only one H of the amino groups in purines is well-documented in the literature [24,25]. Moreover, the increase in the absorbance over the entire spectral region after 110 min of electrolysis during spectral analysis; appears to be due to the formation of dimer (**22**), which possesses a highly conjugated π-system due to C–C linkage. The formation of dimers (**18**) and (**20**) as shown in Scheme 2, appears to be due to $1e^-$, $1H^+$ oxidation of 2-hydroxy-2′-deoxyadenosine (**2**) in a side reaction to give a radical species (**17**). The radical species (**17**) dimerizes rapidly with its similar moiety to give a dimer (**18**) having peroxide type of linkage. The dimer (**18**) has eight reactive sites, which can be replaced by trimethylsilyl units on silylation. However, it was observed that under the silylation conditions used only one hydrogen of the amino group at C-6 position was replaced by trimethylsilyl group. A peak at $R_t \sim 9.86$ min in GC–MS chromatogram (*m/z* 964) indicated the formation of the silylated dimer (**19**). The radical species (**17**) also seems to combine with ($\mathbf{1_d}$) to give the corresponding C_8–O–C_2 bridged dimer (**20**). The silylated derivative of dimer (**20**), gave a clear molecular ion (M^+) peak having *m/z* 948 corresponding to the GC–MS peak at $R_t \sim 11.05$ min. Like dimer (**19**) and (**23**) it retains both the deoxyribose sugar moieties and upon silylation at 110 °C both the reactive OH groups from the five membered deoxyribose ring are rapidly silylated. In contrast, the NH_2 group from the adenine base, upon silylation changes to $NHSi(CH_3)_3$ rather than $N[Si(CH_3)_3]_2$. The high molar mass peaks observed in the fragmentation pattern are compiled in Table 3.

3.14.2. In neutral media

The formation of C_8–O–O–C_8 bridged dimer (**26**) and C_8–N_6–C_8 linked trimer (**31**) as the products of the secondary electrode process at pH 7.20 is mechanistically represented in Scheme 3 and their formation can be explained by EC mechanism as follows. The $1e^-$, $1H^+$ oxidation of (**3**) can generate free radical (**24**) at a PGE surface. Such an oxidation at position C_8–OH is well documented [15,23] for adenosine and adenosine 5′-monophosphate. The free radical (**24**) generated from (**3**) rapidly dimerizes with a similar moiety to form C_8–O–O–C_8 bridged dimer (**25**). It is interesting, to observe that both the deoxyribosyl moieties of dimer (**25**) hydrolyze during silylation, which has also been observed earlier by several workers [25] and [26]. The GC–MS peak at $R_t \sim 9.952$ min with *m/z* 908 (M^+) corresponds to the octasilylated derivative of the dimer (**25**) having C_8–O–O–C_8 linkage in which the NH_2 group from the adenine base, upon silylation changes to $N[Si(CH_3)_3]_2$ due to the loss of the sugar units (**26**). The formation of the second product, trimer (**30**), during secondary reactions of the electrooxidation of 2′-deoxyadenosine (**1**) can be accounted for, on the basis of the combination of radical species ($\mathbf{1_a}$) and ($\mathbf{1_d}$) at the electrode surface, forming a reactive dimer (**27**). The $1e^-$, $1H^+$ oxidation of (**27**) is expected to produce a radical (**28**) having an odd electron at N-1 atom of the dimer (**27**). The free radical species (**28**) generated during the process of oxidation, upon combination with a radical species ($\mathbf{1_d}$), yields a trimer (**30**) having a C_8–N_6–C_8 linkage and in which two deoxyribose sugar units have been hydrolyzed in aqueous solution probably, due to the steric hindrance caused by the deoxyriboside moieties during dimerization. The hydrolysis of the deoxyribosyl bond during electrooxidation of purines and purines nucleosides is well reported in the literature [15,27]. This trimer obtained as one of the products of the electrooxidation was identified as its hexasilylated derivative (**31**) having *m/z* 949 by GC–MS. The peak obtained in the GC–MS chromatogram at $R_t \sim 17.957$ min corresponds to $M+H^+$ peak having *m/z* 950.

Schemes 1, 2 and 3 suggest the most probable routes for the formation of various products, however, it must be realized that more than one pathways are always possible for the formation of these products. The formation of oxidative free radicals and dimeric purine moieties have been detected in oxidized DNAs by many worker [28]. Hence, on the basis of such studies it can be concluded that 2′-deoxyadenosine is also oxidized in biosystems, leading to the formation of several dimers / trimers.

4. Conclusion

The present studies clearly reveal that the electron transfer reactions of 2′-deoxyadenosine at the electrode surface occurs by pathway much more complicated than observed for the

corresponding purine nucleoside, adenosine. To monitor the effect of deoxyribose moiety on the oxidation behavior, a comparison was made with the electrooxidative pathway of adenosine. The $6e^-$, $6H^+$ oxidation of 2′-deoxyadenosine has been found to occur in three $2e^-$, $2H^+$ steps via a mechanism similar to that proposed for adenosine. Moreover, a free radical mechanism is also observed to play a significant role during oxidation of 2′-deoxyadenosine. The ultimate products of oxidation of adenosine in acidic and neutral pH were alloxan and C_8–O–O–C_8 bridged dimer. On the other hand, oxidation of 2′-deoxyadenosine gave alloxan, C_8–C_8, C_8–O–C_2, C_2–O–O–C_2 bridged dimers in acidic media and allantoin, C_8–O–O–C_8 linked dimer, C_8–N_6–C_8 bridged trimer at neutral pH. The formation of alloxan and C_8–O–O–C_8 dimer in case of oxidation of 2′-deoxyadenosine, essentially occurs via a pathway similar to that proposed for adenosine, including, several hydrolysis step whereas the formation of other oxidative products (dimers, trimers) during 2′-deoxyadenosine oxidation, occurred through the various combination of the free radicals generated during electron transfer reactions at the electrode-solution interface. Thus, the deoxyribosyl moiety significantly affects the mechanism of electrode reaction and probably causes the reaction to proceed via free radical mechanism along with the primary electrode reactions. Thus, it can be concluded on the basis of these investigations that 2′-deoxyadenosine is also oxidized in biosystems leading to the formation of several products, which could serve as an important tool for the biochemists to deeply understand the medicinal applications of the products formed under oxidative conditions in the human physiology. Overall, mechanistic pathway of 2′-deoxyribonucleoside of adenine can serve as a perfect model to enlighten the complex biological reactions occurring at the enzyme-solution interface in the biosystem.

Acknowledgement

A. Dhawan is thankful to the University Grant Commission, New Delhi for the award of Junior Research Fellowship and partial financial assistance for the work was also provided by the Council of Scientific and Industrial Research, New Delhi vide grant No. 01 (1815)/ 02/ EMR-II.

Appendix A. Supplementary data

Supplementary data associated with this article can be found, in the online version, at doi:10.1016/j.bioelechem.2006.03.003.

References

[1] G. Dryhurst, Electrochemistry of Biological Molecules, Academic Press, New York, 1977, p. 74.
[2] F.A. Fuhrman, G.J. Fuhrman, Effects of some naturally occurring purine ribosides on purinergic receptors in cardiac and smooth muscle, Comp. Biochem. Physiol. 72 (1982) 203–210.
[3] K. Fabianowska-Majewska, J.A. Duley, H. Ann Simmonds, Effects of novel antiviral adenosine analogues on the activity of *S*-adenosylhomocysteine hydrolase from human liver, Biochem. Pharmacol. 48 (1994) 897–903.
[4] E. Bojarska, B. Czochralska, Electrooxidation of the antileukemic 2-chloro-2′-deoxyadenosine and related compounds, J. Electroanal. Chem. 477 (1999) 89–96.
[5] J. Barankiewicz, E. Abushanab, L. Makings, A. Danks, T. Wiemann, T. Fox, P. Marangos, Regulation of adenosine concentrations and attenuation of ischemia by novel reversible ADA inhibitors, Clin. Biochem. 30 (1997) 299.
[6] A.R. Wakade, J.S. Kulkarni, J.T. Fujii, 2′-deoxyadenosine selectively kills nonneuronal cells without affecting survival and growth of chick dorsal root ganglion neurons, Brain Res. 788 (1998) 69–79.
[7] S. Frelon, T. Douki, Radical oxidation of the adenine moiety of nucleoside and DNA: 2-hydroxy-2′-deoxyadenosine is a minor decomposition product, Free Radic. Res. 36 (2002) 499–508.
[8] T. Sengupta, S.D. Choudhury, S. Basu, Medium-dependent electron and H atom transfer between 2′-deoxyadenosine and menadione: a magnetic field effect study, J. Am. Chem. Soc. 126 (2004) 10589–10593.
[9] I.D. Podmore, D. Cooper, M.D. Evans, M. Wood, J. Lunec, Simultaneous measurement of 8-oxo-2′-guanosine and 8-oxo-2′-deoxyadenosine by HPLC-MS/MS, Biochem. Biophys. Res. Commun. 277 (2000) 764–770.
[10] F.J. Miller, H.E. Zittel, Fabrication and use of pyrolytic graphite electrode for voltammetry in aqueous solutions, Anal. Chem. 35 (1963) 1866–1869.
[11] G.D. Christian, W.C. Purdy, Residual current in orthophosphate medium, J. Electroanal. Chem. 3 (1962) 363–367.
[12] J.J. Lingane, Electroanalytical Chemistry, 2nd ed., Wiley, New York, 1968, p. 222.
[13] T.R. Chen, G. Dryhurst, Oxidation chemistry of 3,7-dimethyluric acid: electrochemical and peroxidase-catalyzed mechanisms, J. Electroanal. Chem. 177 (1984) 149–165.
[14] R.H. Wopshall, I. Shain, Effects of adsorption of electroactive species in stationary electrode polarography, Anal. Chem. 39 (1967) 1514.
[15] R.N. Goyal, A. Sangal, Electrochemical investigations of adenosine at solid electrodes, J. Electroanal. Chem. 521 (2002) 72–80.
[16] Vogel′s, Textbook of practical organic chemistry, ELBS with Longman, UK, 1994, pp. 402.
[17] D. Swern, Organic Peroxides, Wiley Interscience, New York, 1971.
[18] R.N. Goyal, A. Kumar, A. Mittal, Oxidation chemistry of adenine and hydroxyadenines at pyrolytic graphite electrodes, J. Chem. Soc., Perkin Trans. 2 (1991) 1369–1375.
[19] H. Kamiya, H. Kasai, Formation of 2-hydroxydeoxyadenosine triphosphate, an oxidatively damaged nucleotide, and its incorporation by DNA polymerases. Steady-state kinetics of the incorporation, J. Biol. Chem. 270 (1995) 19446–19450.
[20] R.N. Goyal, N.K. Singhal, Voltammetric and chronoamperometric investigations on the oxidation of 7-methylxanthine, Indian J. Chem. 38 A (1999) 49–55.
[21] J. Wang, X. Cai, J.Y. Wang, C. Jonsson, E. Palecek, Trace measurements of RNA by potentiometric stripping analysis at carbon paste electrodes, Anal. Chem. 67 (1995) 4065–4070.
[22] R.N. Goyal, N. Jain, D.K. Garg, Electrochemical and enzymic oxidation of guanosine and 8-hydroxyguanosine and the effects of oxidation products in mice, Bioelectrochem. Bioenerg. 43 (1997) 105–114.
[23] R.N. Goyal, A. Sangal, Electrochemical oxidation of adenosine monophosphate at a pyrolytic graphite electrode, J. Electroanal. Chem. 557 (2003) 147–155.
[24] R.N. Goyal, A.K. Jain, N. Jain, Electrochemical and peroxidase catalyzed oxidation of 1,7-dimethyluric acid and effect of methyl groups on the oxidation mechanism, J. Chem. Soc., Perkin Trans. 2 (6) (1996) 1153–1159.
[25] R.N. Goyal, A. Brajter-Toth, J.S. Besca, G. Dryhurst, The electrochemical and peroxidase-catalyzed redox chemistry of 9-β-D-ribofuranosyluric acid, J. Electroanal. Chem. 144 (1983) 163–190.
[26] A.A. Rostami, G. Dryhurst, Electrochemical oxidation of 6,8-dioxypurine, electrochemical oxidation of 6,8-dioxypurine, J. Electroanal. Chem. 223 (1987) 143–160.
[27] R.N. Goyal, S.M. Sondhi, A.M. Lahoti, Investigations of electron-transfer reactions and the redox mechanism of 2′-deoxyguanosine-5′-monophosphate using electrochemical techniques, New J. Chem. 29 (2005) 587–595.
[28] N.J. Duker, J. Sperling, K.J. Soprano, D.P. Druin, A. Davis, R. Ashworth, Beta-Amyloid protein induces the formation of purine dimers in cellular DNA, J. Cell. Biochem. 81 (2001) 393–400.